Published in final edited form as:
Cancer Res. 2013 August 1; 73(15): 4791–4800. doi:10.1158/0008-5472.CAN-13-0587.

Enhanced radiation sensitivity in HPV-positive head and neck cancer

Randall J. Kimple, MD PhD[1,3], **Molly A. Smith, BS**[1], **Grace C. Blitzer, BS**[1], **Alexandra D. Torres, BS**[1,2], **Joshua A. Martin, BS**[1,2], **Robert Z. Yang, MD**[1,2], **Chimera R. Peet, PhD**[1], **Laurel D. Lorenz, BSC**[2], **Kwangok P. Nickel, PhD**[1], **Aloysius J. Klingelhutz, PhD**[4], **Paul F Lambert, PhD**[2,3], and **Paul M. Harari, MD**[1,3]

[1]Department of Human Oncology, University of Wisconsin, Madison, WI, USA

[2]McArdle Laboratory for Cancer Research and Department of Oncology, University of Wisconsin, Madison, WI, USA

[3]University of Wisconsin Carbone Cancer Center, University of Wisconsin, Madison, WI, USA

[4]Department of Microbiology, University of Iowa, Iowa City, IA, USA

Abstract

Patients with human papillomavirus associated (HPV+) head and neck cancer (HNC) demonstrate significantly improved survival outcome compared to those with HPV− negative (HPV−) tumors. Published data examining this difference offers conflicting results to date. We systematically investigated the radiation sensitivity of all available validated HPV+ HNC cell lines and a series of HPV− HNC cell lines using in vitro and in vivo techniques. HPV+ HNCs exhibited greater intrinsic radiation sensitivity (average SF2 HPV− 0.59 vs. HPV+ 0.22, p<0.0001), corresponding with a prolonged G2/M cell cycle arrest and increased apoptosis following radiation exposure (percent change 0% vs. 85%, p=0.002). A genome-wide microarray was used to compare gene-expression 24 hours following radiation between HPV+ and HPV− cell lines. Multiple genes in *TP53* pathway were upregulated in HPV+ cells (Z score 4.90), including a 4.6 fold increase in *TP53* (p<0.0001). Using immortalized human tonsillar epithelial cells, increased radiation sensitivity was seen in cell expressing HPV-16 E6 despite the effect of E6 to degrade p53. This suggested that low levels of normally functioning p53 in HPV+ HNC cells could be activated by radiation, leading to cell death. Consistent with this, more complete knockdown of *TP53* by siRNA resulted in radiation resistance. These results provide clear evidence, and a supporting mechanism, for increased radiation sensitivity in HPV+ HNC relative to HPV− HNC. This issue is under active investigation in a series of clinical trials attempting to de-escalate radiation (and chemotherapy) in selected patients with HPV+ HNC in light of their favorable overall survival outcome.

Keywords

Head and neck cancer; human papillomavirus; HPV; DNA tumor viruses; radiation

Corresponding Author: Randall J Kimple, MD PhD, Department of Human Oncology, University of Wisconsin Comprehensive Cancer Center, 3107 WIMR, 1111 Highland Avenue, Madison, WI 53705. Phone: (608) 265-9156, Fax: (608) 263-9947, rkimple@humonc.wisc.edu.

Conflicts of Interest: none

Introduction

Human papillomavirus (HPV) plays a central etiologic role in an expanding subset of head and neck cancer (HNC) patients (1, 2). Clinical reports provide clear evidence of improved outcome in patients with HPV-positive (HPV+) HNC versus HPV-negative (HPV−) tumors (3, 4). This result that has been postulated to reflect increased radiation sensitivity in HPV+ tumors (5). However, published results for the few HPV+ cancer cell lines investigated to date are conflicting with some data suggesting enhanced sensitivity to radiation and some suggesting reduced sensitivity or no effect (6-9). The strength of these data are somewhat limited due to the model systems used: p53 mutated cells, non-head and neck cancer cell lines, and absence of rigorous validation of HPV status. Clarification of this discrepancy is important to clinical investigators as they consider future clinical trials that incorporate radiation dose reduction and seek underlying mechanisms to explain the markedly improved survival outcomes observed in patients with HPV+ HNC.

The classical HPV− HNC, related to more traditional risk factors such as tobacco and/or alcohol exposure, is driven by a series of mutations in tumor suppressor genes and proto-oncogenes. While many of these mutations occur randomly, recent next-generation sequencing approaches have identified mutations in common genes or their resultant protein pathways including *TP53, NOTCH, PIK3CA*, and *CDKN2A* (10-12). In fact, it is estimated that approximately 80% of HPV-negative (HPV−) HNCs harbor mutations in *TP53* resulting in impaired or absent function of its encoded protein p53 (10-12).

Alternatively, during the development of HPV+ HNC, an initial viral infection results in expression of virally encoded oncogenes that can have dramatic effects on normal host cellular function. Canonically, the HPV proteins E6 and E7 down regulate the tumor suppressor proteins p53 and Rb, respectively, although their true interactome encompasses a wide variety of cellular targets (13). Recent work has shown that the E6 and E7 proteins act synergistically to induce HNC in a transgenic mouse model system and that additional targets (e.g. p107 and p130) besides Rb are targeted by E7(14-16). This coordinated perturbation of two critical tumor suppressor pathways results in uncontrolled growth and proliferation although with a mutational landscape that is significantly restricted when compared to HPV− HNC (10-12).

Standard therapy for patients with locally advanced HNC commonly involves the combination of radiation and cisplatin chemotherapy. Surgery is often incorporated either in the initial management or as salvage following definitive radiochemotherapy (reviewed in (17)). In 2013, despite the significant differences in underlying biology and ultimate outcome, there are no validated differences in treatment approach based on HPV status, beyond the context of clinical trials. In addition, there is little preclinical data to support a given treatment approach owing, at least in part, to the lack of preclinical model systems of HPV+ HNC.

During the last two years, we have systematically investigated the therapeutic sensitivity of a panel of validated HPV+ and HPV− HNC cell lines, in an effort to generate preclinical data to support etiology-specific treatment approaches. As consistent differences in radiation sensitivity between HPV+ and HPV− cells were identified, we sought to further investigate mechanisms underlying these altered responses and to validate the findings in an in vivo model system.

Methods

Cell lines and culture conditions

Head and neck cancer lines derived from HPV− patients: UM-SCC1, UM-SCC6, UM-SCC22B, and SCC-1483 and from HPV+ patients: UD-SCC2, UM-SCC47, UPCI-SCC90, and 93-VU-147T were obtained from indicated sources (Supplemental Table 1). Standard culture conditions were used (Supplemental Table 1). The identity of all cell lines was confirmed via short tandem repeat testing within 6 months of cell use.

Immortalized human tonsillar epithelial (HTE) cells were generated by co-transduction of primary HTE cells with a pBABE-Hygro-TERT retroviral vector (a gift from Dr. Robert Weinberg) and a shRNA-p16-Puro-MSCV retroviral vector (a gift from Dr. Scott Lowe) using transduction techniques as previously described (18). HTE cells stably carrying LXSN vector alone, or engineered to encode *HPV16 E6, E7* or *E6* and *E7* were cultured in keratinocyte serum free media (Cat # 17005042, Invitrogen, Carlsbad, CA) supplemented with 0.16 ng/ml EGF and 25 μg/ml Bovine Pituitary Extract at 37°C in a humidified atmosphere of 5% $C0_2$.

Validation of HPV

Southern blot was performed using 10 μg of BamHI digested total cellular DNA. DNA was separated on a 1.25% agarose gel, transferred to Hybond N+ nylon membrane (Amersham, Pittsburgh, PA) and crosslinked. DNA probes were made by 5′ end labeling 10 pmoles of HPV16 specific oligonucleotides (Supplemental Table 2) in the presence of T4 polynucleotide kinase (New England Biolabs Inc., Ipswich, MA) with [γ-^{32}P] ATP (6,000 Ci/mmol) at 37°C for 1.5 hours. The membrane was pre-hybridized with Church hybridization buffer for 15 minutes at 52°C followed by probe hybridization for 18 hours at 52°C in a hybridization oven. Membrane was washed with Church wash buffer, exposed to a storage phosphor screen and scanned using a Typhoon 8610 imaging system (Amersham).

Quantitative reverse-transcriptase PCR (qRT-PCR) was performed to confirm transcription of *HPV-16 E5, E6*, and *E7* on a BioRad CFX96 using primers and probes (Supplemental Table 2) purchased from Integrated DNA Technologies, Inc. (Coralville, IA). Briefly, total RNA was harvested using the miRNeasy with RNeasy MinElute Cleanup Kit (Cat# 217004 and 74204, Qiagen, Valencia, CA) from confluent plates of both HPV+ and HPV− cell lines. cDNA was synthesized using the iScript Reverse Transcription Supermix kit (Bio-Rad Laboratories, Hercules, CA) and 1,000 ng of total RNA. qRT-PCR was performed by using IQ Multiplex Powermix with 10 ng cDNA per 10 μl reaction. *GAPDH, HPV-16 E5, E6, E7* and *TP53* transcripts were detected using primers and probes (Supplemental Table 2) purchased from Integrated DNA Technologies, Inc. (Coralville, IA). The thermocycler was programmed for an initial 95°C for 7 minutes followed by 40 cycles of 94°C for 15 seconds and 60°C for 30 seconds.

Clonogenic survival assays

Clonal survival of cells following radiation was performed as previously described using a JL Shepherd ^{137}Cs irradiator (JL Shepherd, San Fernando, CA) delivering a dose rate of approximately 400 cGy/min (19). After 10 to 15 days, colonies containing more than 50 cells were counted, the surviving fraction calculated, and clonogenic survival curves fit to a linear-quadratic model, as previously described (19). Clonogenic survival curves were compared using the extra sum-of-squares F test in GraphPad Prism version 5.01 (GraphPad Software, San Diego, CA). Each point represents the mean surviving fraction calculated from three independent experiments done in triplicate for each treatment condition; error bars represent the standard deviation.

Cell cycle analysis

Untreated and irradiated cells (4 Gy) were harvested by trypsinization, washed with ice cold PBS, and fixed with 95% ethanol overnight at −20°C prior to DNA analysis. Following removal of ethanol by centrifugation, cells were incubated with PI Master Mix (40 μg/ml propidium iodide and 100 μg/ml RNase in PBS) at 37°C for 30 minutes prior to analysis by FACSCalibur flow cytometry. Stained nuclei were analyzed for DNA/propidium iodide fluorescence and resulting DNA distributions analyzed by Modfit (Verity Software House, Inc. Topsham, ME). Percent change from baseline (unirradiated) is graphed from samples (n=3) collected 4, 24, and 48 hours after radiation.

Immunoblot analysis

Following treatment, cells were lysed with Tween-20 lysis buffer (50 mM HEPES pH 7.4, 150 mM NaCl, 0.1% Tween-20, 10% glycerol, 1 mM EDTA, 1 mM DTT, 1 mM phenylmethylsulfonylfluoride, and 10 μg/ml leupeptic and aprotinin) and sonicated. Equal amounts of protein were analyzed by SDS-PAGE (25 μg – 75 μg depending upon target), proteins were transferred to PVDF membranes, analyzed by specific primary antibodies, detected via incubation with horseradish peroxidase-conjugated secondary antibodies using ECL chemiluminescence detection. Antibodies and sources are listed in Supplemental Table 3.

Apoptosis

Two distinct assays were utilized to assess apoptosis. A luminescent DEVD cleavage assay for Caspase 3/7 activity (ApoTox Triplex Assay, Promega, Madison, WI) was performed in 96-well format. Briefly, cells (2,000/well) were plated in 100 μl media. Plates were irradiated (4 Gy) or mock treated and apoptosis was measured 24, 48, and 72 h after irradiation. Caspase activity was monitored according to the manufacturer's directions and normalized to the total number of cells. Baseline activity was subtracted from each time point and the percent increase over baseline plotted. All experiments were repeated 3 times and graphs represent the mean of 6 individual replicates per experiment. In addition, apoptosis was detected by flow cytometry via the examination of altered plasma membrane phospholipid packing by lipophilic, FITC conjugated Annexin V (Cat# 556547 BD Biosciences San Jose, CA) according to manufacturer directions. Both early (Annexin V positive, propidium iodide negative) and late (both positive) cells as well as live (both negative) cells were detected by FACSCalibur flow cytometry and analyzed by FlowJo v9.4.3 (Tree Star, Inc. Ashland, OR).

Global Gene Expression Analysis

Global gene expression analysis of HPV+ and HPV− cell lines was performed using Affymetrix Gene 1.1 ST Array Plate technology (Affymetrix, Santa Clara, CA). Briefly, cell lines (n=8) were harvested as biologic triplicates after mock therapy or 24 h after a single 4 Gy dose of radiation. Total RNA from each cell line was prepared using Qiagen RNeasy, RNA quality was assessed by bioanalyzer and only samples with a RNA Integrity Number (RIN) >9.0 were utilized. Samples were processed by the University of North Carolina Expression Profiling and SNP Genotyping Core Facility. Normalized data were imported into GeneSifter (Geospiza, Inc. Seattle WA). A pairwise comparison between HPV+ and HPV− cells 24 hrs after radiation with the fold change threshold set to 1.5 was performed. Differences between HPV+ and HPV− cells were viewed by KEGG pathway and compared by t-test with Bonferroni correction.

siRNA knockdown of *TP53*

TP53 specific siRNA, including scrambled control, was purchased from Invitrogen (Silencer Select siRNA, Cat #4390825), transfected into cell lines using Lipofectamine RNAiMax reagent (Invitrogen). Knockdown of p53 was confirmed by western blot. Transfected cells were used 48 hrs after transfection.

Xenografts

Four to five week-old Hsd:athymic Nude-Foxn1^{nu} female mice were purchased from Harlan Laboratories (Madison, WI), housed in filter-topped cages in an aseptic environment, and maintained per defined protocol approved by and in accordance with the University of Wisconsin Animal Care and Use Committee. To establish xenografts, cells (1-2 × 10^6 mixed 1:1 with Matrigel (BD Biosciences, San Jose, CA) were injected subcutaneously into bilateral flanks. When tumors reached approximately 200 mm^3, mice (n=12/group) were randomly assigned to either mock radiation, or 8 Gy delivered in four 2 Gy fractions delivered over two consecutive weeks (Supplemental Materials and Methods). Radiation was delivered using an X-rad 320 biological irradiator (Precision X-ray, Inc., North Branford, CT) using a dose rate of approximately 0.6 Gy/min with customized lead immobilization jigs to shield the majority of the mouse body while leaving the tumor exposed. Tumors were measured, growth curves generated, and comparisons using the extra sum-of-squares f-test, as previously described (19). Time to tumor quadrupling was calculated from the first day of treatment, graphed according to the method of Kaplan and Meier and compared using the log-rank (Mantel-Cox) test using GraphPad Prism.

RESULTS

Validation of HPV status

Following receipt of several HNC cell lines reported to contain HPV that showed no detectable HPV DNA, we were concerned about a potential divergent cell population. Thus, we performed single cell isolation and clonal selection of all HPV+ HNC cell lines by plating <1 cell/well, visually confirming the presence of single small colonies with subsequent expansion to a uniform population of cells. All experiments herein utilized these clonally isolated cellular populations.

Southern blot was used to confirm the presence of HPV DNA in the HPV+ cell lines (UD-SCC2-C6, UM-SCC47-C3, UPCI-SCC90-C35, and 93-VU-147T-C5) and the absence of HPV in the HPV− cell lines (Figure 1A). Differences in the restriction digest pattern result from different patterns of integration and was confirmed to match that previously published (20-22). The UD-SCC2 cell line had no known Southern blot published, but karyotype analysis confirmed a population distribution (data not shown) similar to that previously described (23). In addition, qRT-PCR was used to confirm the presence or absence of *HPV16 E6* and *HPV16 E7* gene expression in HPV+ and HPV− cells, respectively (Figure 1B).

Increased radiation sensitivity in HPV+ HNC

We utilized our panel of eight HNC cell lines to investigate radiation sensitivity using clonogenic survival assays. A wide range of sensitivity was seen across cell lines with the surviving fraction after 2 Gy (SF2) ranging from 0.11 to 0.73 (Figure 1C). HPV+ cell lines showed a significantly greater sensitivity to radiation as shown by average SF2 (HPV−: 0.59 vs. HPV+: 0.22, $p<0.0001$).

Altered cell cycle arrest in HPV+ HNC

The HPV oncoproteins E6 and E7 can have profound effects on cell cycle regulation (24). To examine whether baseline cell cycle distribution might contribute to the increased radiation sensitivity observed in HPV+ HNC cells, we used propidium iodide staining to assess baseline and post-radiation cell cycle distribution. At baseline, no difference in cell cycle distribution was seen between HPV+ and HPV− cells (Figure 2A, inset, p=ns for G1, G2, and S).

Interestingly, significant differences between HPV+ and HPV− cells were seen in their cell cycle distribution in response to radiation. Compared to unirradiated cells, a significant increase in cells in the G2 fraction was seen 24 hrs after a single 4 Gy dose of radiation (Figure 2A, p=0.0006 for HPV+ vs. HPV−). The G2 arrest was not only greater in magnitude in HPV+ cells, but was also of longer duration with a significant difference in the proportion of cells in G2, 48 hrs after radiation ($p<0.0001$). Consistent with this finding, both cyclin B1 and phospho-CDK2 show upregulation in HPV+ cells following a single 4 Gy dose of radiation (Figure 2B). In both cases, this upregulation was greater 24 hrs after radiation than 4 hrs after radiation consistent with the prolonged G2/M arrest seen in cell cycle analysis. Cyclin E, a marker of G1/S remained relatively unchanged in HPV+ cell lines at these same time points.

Increased apoptosis in HPV+ HNC

Clinically, patients with HPV+ HNC are reported to demonstrate earlier tumor response than those with HPV− HNC (25). This kinetic profile has been associated with apoptotic tumor responses in other types of cancers (26). A caspase activity assay was used to assess apoptosis in HPV+ and HPV− cell lines treated by radiation. While HPV− cells showed only slight increases in apoptosis, HPV+ cells showed robust induction of apoptosis (Figure 3A). On average, 24 hrs after a single 4 Gy dose of radiation HPV− cells showed no increased in caspase activity while HPV+ cells showed an 85% increase (p=0.002). Apoptosis was also assessed by Annexin V labeling and flow cytometry in HPV+ cells. A significant increase in the percentage of cells positive for Annexin V was seen in 3 of 4 HPV+ cell lines (Figure 3B). The single cell line with little increase in Annexin V staining was 93-VU-147T. This cell line showed the lowest radiation sensitivity (Figure 1), and relatively small increases in G2 fraction (Figure 2A), and small increases in caspase activity (Figure 3A) following radiation. Interestingly, although it has been reported to harbor wild-type p53 (27), in our hands this cell line was found to have a heterozygous mutation in p53 (c.770T>G, p.L257R, data not shown). All other HPV+ cell lines contain wild-type p53 (21, 27, 28).

Activation of p53 in HPV+ cell lines

As there are significant differences between HPV+ and HPV− HNC in terms of global gene expression (24), we performed Affymetrix microarrays on our panel of eight HPV+ and HPV− HNC cell lines. While a full, unsupervised analysis is ongoing, based upon KEGG analysis, multiple genes in the *TP53* pathway were significantly different between HPV+ and HPV− cells 24 hrs after radiation (Z score 4.90). For example, levels of *TP53* RNA were increased 4.63 fold in HPV+ vs. HPV− cells at baseline ($p<0.0001$). Using qRT-PCR of irradiated samples, levels of *TP53* RNA were further increased following radiation in HPV+ vs. HPV− cell lines (Figure 4A).

To determine whether these differences in gene expression resulted in alterations in protein levels, we harvested cellular lysates at baseline, 4, and 24 hr after radiation and assessed levels of p53 and activated, phosphorylated-p53. Absolute levels of p53 varied significantly at baseline such that multiple exposures and ECL reagents were required to identify any p53 protein in UM-SCC47. As expected in a normal epithelial cell line, increased total and

phospho-p53 was observed in HTE cells (Figure 4B, left). While p53 responses in cancer cells can differ from those in normal cells, an increase in activated, phosphorylated-p53 was seen in UM-SCC47, UPCI-SCC90, and 93-VU-147T following radiation (Figure 4B, right). An increase in total p53 was also seen at these selected time points following radiation in UPCI-SCC90. In HPV− cells, no appreciable p53 was identified in UM-SCC1, UM-SCC6, or UM-SCC22B while SCC1483 showed a slight induction of p53, 4 and 24 hrs after radiation (data not shown). Consistent with activation of p53 by radiation, p21 RNA was increased following radiation compared to baseline in 3 of 4 HPV+, but only 1 of 4 HPV−, HNC cell lines (Figure 4F).

Increased radiation sensitivity related to HPV E6 expression

To investigate the individual contributions of HPV oncoproteins, we utilized a unique system of immortalized human tonsillar epithelial (HTE) cells. Cells stably carrying *pLXSN* vector alone (+LXSN), or encoding either *pLXSN-HPV-16 E6* (+16E6) or *pLXSN-HPV-16 E6* and *E7* (+16E6E7) were used to perform colony formation assays. A decrease in clonogenic survival (corresponding to increased sensitivity to radiation) was seen in both 16E6 and 16E6E7 expressing cells (Figure 4C). Interestingly, little increase in the G2 fraction was seen in HTE-16E6 cells while expression of both E6 and E7 resulted in a significant G2 arrest (Figure 4D) as seen in the patient derived SCC cell lines. Both E6 and E6/E7 resulted in an increase in apoptosis as measured by caspase activity (Figure 4E).

Knockdown of TP53 results in radiation resistance

We hypothesized that the wild type TP53 present in the +16E6 and +16E6E7 cells was being reactivated following radiation resulting in improved sensitivity to radiation. To test this hypothesis we performed siRNA-mediated knockdown of p53 in our HTE +16E6 cell line in addition to using two HPV+ HNC cell lines. As expected, compared to vector alone, expression of 16E6 resulted in a decrease in detectable p53 (Figure 5A). Use of a *TP53* specific siRNA, but not vehicle or scrambled control siRNA, led to a further reduction in p53 expression to levels that were undetectable (Figure 5A). Similar decreases in total p53 were seen in 93-VU-147T and UM-SCC47 cells treated with the same siRNA, but not with scrambled control siRNA (data not shown). Using clonogenic survival assays, treatment with scrambled siRNA resulted in a survival fraction similar to that previously seen in untreated cells (Figure 1C and 4C). Use of *TP53* specific siRNA resulted in a significant increase in colony formation consistent with radiation resistance in HTE +16E6, UM-SCC47, and 93-VU-147T cells (Figure 5B).

In vivo radiation sensitivity

To determine whether the increased radiation sensitivity seen in vitro was also present in vivo, we utilized a cell line xenograft system. All four HPV+ cell lines (Figure 6A) and all 4 HPV− cell lines (data not shown) were grown as flank-implanted xenografts. An initial dose-finding experiment was performed with UM-SCC47 and a dose/fractionation schedule of 2 Gy delivered twice weekly to a total dose of 8 Gy was adopted for all subsequent experiments. Even this relatively low radiation dose resulted in significant tumor growth delay in 3 of 4 HPV+ cell lines (Figure 6A). However, the relatively rapid tumor growth rate, coupled with the prolonged time interval between radiation fractions, elicited no overall tumor regression in these xenografts. When a higher daily dose (4 Gy per fraction) was utilized in the UM-SCC47 cell line, modest tumor regression was seen (data not shown). Interestingly, the slowest growing line, 93-VU-147T, demonstrated modest tumor regression in the irradiated tumors, but overall tumor growth was not significantly different after 100 days.

To determine whether a significant difference in populations was seen, time to tumor quadrupling from the first day of treatment was calculated for all eight xenografts. No significant difference in median time to tumor quadrupling was seen between control (mock radiation) treated HPV+ and HPV− tumors (p=0.68, data not shown). In HPV− xenografts, no difference between control and radiated tumors was seen (Figure 6B, p=0.14). However, consistent with increased radiation sensitivity in HPV+ HNC, xenografts of HPV+ cells showed a significant prolongation in time to tumor quadrupling between control and irradiated tumors (Figure 6C, p=0.0003).

DISCUSSION

In early publications suggesting an etiologic link between HPV and HNC, Gillison and colleagues postulated that HPV+ HNC may be more sensitive to radiation than HPV− HNC (1). More recently, clinical trial data demonstrates that patients with HPV+ HNC have markedly improved tumor control and survival outcomes when treated with radiation, and indeed with other treatment approaches (3, 4). However, the very limited experimental data that currently exists is conflicting. For example, one group demonstrated increased radiation sensitivity in two putatively HPV+ cell lines compared to one HPV− cell line (6), while a second report showed decreased radiation sensitivity for the same HPV+ cells compared to three different HPV− cells (7). Cells obtained directly from this group did not confirm the presence of HPV DNA, highlighting the critical importance of confirming the presence of viral DNA in cells during their use. Whether this resulted from loss of viral DNA, selection of a non-viral DNA-containing clonogen, or cell culture contamination is unclear, but may explain the discrepant results previously reported (6, 7). The uncertainty regarding the HPV status in the few globally available HPV+ HNC cell lines led us to acquire cells directly from the original labs that generated them, and perform Southern blot analysis to confirm the presence of viral DNA. In addition, due to concern regarding potentially mixed population of cells, we performed single cell isolation and confirmed the presence of integrated HPV and expression of viral oncogenes in the isolated cell clones. Only these individually cloned cell lines, which we revalidated by Southern to contain HPV16 with integration patterns or karyotypic properties consistent with the original reported lines, were used in the current study.

Using these well-validated clonal HPV+ HNC cell lines, we demonstrate that they are consistently more sensitive to radiation than HPV− HNC cells both in vitro and in vivo. As expected, there is considerable variation in radiation sensitivity in both HPV+ and HPV− cells. This is certainly true in the clinical domain where HNC patients exhibit a broad spectrum of response to radiation, and we would therefore anticipate a broad response heterogeneity in the preclinical setting as well. Nevertheless, our systematic evaluation of all existing HPV+ HNC cell lines appears to demonstrate a strong pattern of increased radiosensitivity compared with HPV− HNC cell lines. This difference could result in a significant improvement in tumor control probability for HPV+ HNC when compounded over 6-7 weeks of treatment. Radiation sensitivity appears to associate with prolonged radiation-induced G2 cell cycle arrest in HPV+ HNC cells and with increased apoptosis mediated through activation of p53 signaling.

We propose a model (Figure 7) in which titration of the levels of p53 expression plays a critical role in regulating therapeutic response. In the development of HPV− HNC, *TP53* or members of its pathway are commonly mutated, preventing a normal response to radiation induced DNA damage. However, in HPV+ HNC, the HPV-16 E6 oncoprotein induces degradation of p53, an effect that plays a critical role in the induction of cancer but that also removes selective pressure to develop mutations in *TP53* or p53-response pathways. Our data suggests that low levels of wild type, normally functioning, p53 remain in HPV+ cell

lines despite the downregulating effects of E6, and that this p53 can be activated by therapeutic stress such as radiation. This apparently protective response of p53 can be overcome by more complete knockdown of p53 by siRNA. We believe that this response results in prolonged G2 arrest, a result likely augmented by the known additional effects of HPV E6 and E7 to bypass G1 checkpoint control (reviewed in (29)). Finally, perhaps due to a failure of HPV+ cells to repair DNA damage, cells eventually undergo cell death by apoptosis.

Interestingly, both E6 and E7 are involved in activation and repression of DNA damage response pathways to support viral genome maintenance and amplification in the normal viral life cycle. Further understanding of how these alterations are regulated in HPV-induced cancers may shed additional light on the mechanisms of DNA damage repair from therapeutically induced DNA damage.

Several additional studies have investigated the effects of HPV proteins on radiation sensitivity outside of the head and neck. DeWeese and colleagues showed no effect of E6 or E7 on radiation sensitivity in a study using human colon cancer cell lines (9), while Hampson et al. utilized cervical cancer cells engineered to overexpress the HPV oncoproteins and showed that E6 induces radiation resistance in a cell line containing mutant *TP53* (30). It is quite likely that the effects of HPV vary based on the cell of origin and that results obtained in colon or cervical cancer may differ from that in head and neck cancer. In fact, clinical data in anal cancer and cervical cancer, two malignancies induced by HPV and treated primarily with radiation and concomitant chemotherapy, is suggestive of exactly this phenomenon: target radiation doses for patients with anal cancer are in the range of 40-50 Gy (31), while patients with cervical cancer are treated with radiation doses of 70-80 Gy (32).

We believe that this data has important clinical implications providing supportive data for carefully designed studies investigating the role of therapy de-escalation in patients with HPV+ HNC. While current non-surgical therapy approaches for these patients most commonly involves concurrent radiation with either cisplatin, or cetuximab, it may be that alternative regimens involving accelerated radiation or alternative concurrent therapies may be preferable. Ongoing studies including those by the Radiation Therapy Oncology Group and by a number of institutions specifically enrolling patients with HPV+ HNC will provide further insight in this regard. Judicious use of these and novel model systems such as a primary tumorgraft system we have recently reported(33) may be able to provide preclinical data supportive of specific interventions. In addition, it is hoped that understanding the role of p53 and other pathways in the radiation response of HPV+ HNC will provide insights into methods to optimize therapy for patients with HPV− HNC. For example, consistent with our results, PRIMA-1, a molecule with the ability to reactivate mutated p53 may have a role in improving outcomes in patients with HPV− HNC(34).

We acknowledge several limitations of our work. Importantly, the in vivo work has been performed using mice with a compromised immune system. Thus, differences observed in radiosensitivity in vitro and in vivo in our study reflect the inherent radiation sensitivity difference between HPV+ and HPV− HNC cells that is not dependent upon immune surveillance. Spanos and colleagues have suggested that tumor control of mouse tonsillar epithelial cells expressing the human HPV16 E6 and E7 proteins is improved in an immunocompetent mouse compared to a RAG knockout mouse with a compromised immune system (7). It may well be that the presence of a robust immune response further increases tumor control of HPV+ HNC thus magnifying differences in intrinsic radiation sensitivity. However, the consistent findings from both in vitro clonogenic survival assays and in vivo tumor growth delay assays provide support to our conclusions that would not be

possible with only one of the chosen systems. In addition, while there are now thousands of HPV+ HNC patients and biopsy specimens available, there are only a handful of documented HPV+ HNC cell lines available worldwide. We solicited and studied all available cell lines when we commenced this study, but the scarcity of established HPV+ tumor cell lines raises an important question as to why it has been so challenging to isolate and propogate HNC cell lines from patients with HPV+ tumors. Much akin to the rarity of Epstein Barr virus positive cell lines in nasopharynx cancer, the limited number of HPV+ cell lines hampers progress to investigate new therapeutic approaches for these cancer patients. In light of this limitation, we have recently established a patient derived xenograft model system from patients with HPV+ HNC (33) and are hopeful that similar approaches may provide additional insights into the biology of these unique tumors.

In summary, we have shown that compared to HPV− HNC cells, those derived from HPV+ HNC demonstrate increased intrinsic sensitivity to radiation. This is associated with prolonged activation of markers of DNA damage, E6- and E7-mediated radiation-induced G2 arrest, and a strong apoptotic response. It appears that residual wild-type p53 plays an important role in modulating this radiation response as further decrease in p53 results in a loss of radiation sensitivity akin to that seen in HPV− cells. Future studies will investigate the role of HPV-proteins in modulating DNA damage repair and understanding the impact of concurrent radiation and chemotherapy on HPV+ HNC.

Supplementary Material

Refer to Web version on PubMed Central for supplementary material.

Acknowledgments

Financial support and disclosures: Supported by Kaye Fellowship in Head and Neck Cancer Research (RK), Radiological Society of North American Research Fellow Grant (RK), AACR/Bristol Myers Squibb Fellowship in Clinical Cancer Research (RK), K99 CA160639 (RK), R01 CA 113448 (PH), R01 DE017315 (PL).

References

1. Gillison ML, Koch WM, Capone RB, Spafford M, Westra WH, Wu L, et al. Evidence for a causal association between human papillomavirus and a subset of head and neck cancers. J Natl Cancer Inst. 2000; 92:709–20. [PubMed: 10793107]
2. Chaturvedi AK, Engels EA, Anderson WF, Gillison ML. Incidence Trends for Human Papillomavirus-Related and -Unrelated Oral Squamous Cell Carcinomas in the United States. J Clin Oncol. 2008; 26:612–9. [PubMed: 18235120]
3. Rischin D, Young RJ, Fisher R, Fox SB, Le QT, Peters LJ, et al. Prognostic significance of p16INK4A and human papillomavirus in patients with oropharyngeal cancer treated on TROG 02.02 phase III trial. J Clin Oncol. 2010; 28:4142–8. [PubMed: 20697079]
4. Fakhry C, Westra WH, Li S, Cmelak A, Ridge JA, Pinto H, et al. Improved Survival of Patients With Human Papillomavirus-Positive Head and Neck Squamous Cell Carcinoma in a Prospective Clinical Trial. J Natl Cancer Inst. 2008; 100:261–9. [PubMed: 18270337]
5. Lindel K, Beer KT, Laissue J, Greiner RH, Aebersold DM. Human papillomavirus positive squamous cell carcinoma of the oropharynx: a radiosensitive subgroup of head and neck carcinoma. Cancer. 2001; 92:805–13. [PubMed: 11550151]
6. Gupta AK, Lee JH, Wilke WW, Quon H, Smith G, Maity A, et al. Radiation Response in Two HPV-Infected Head-and-Neck Cancer Cell Lines in Comparison to a Non-HPV-Infected Cell Line and Relationship to Signaling Through AKT. International Journal of Radiation Oncology*Biology*Physics. 2009; 74:928–33.

7. Spanos WC, Nowicki P, Lee DW, Hoover A, Hostager B, Gupta A, et al. Immune response during therapy with cisplatin or radiation for human papillomavirus-related head and neck cancer. Arch Otolaryngol Head Neck Surg. 2009; 135:1137–46. [PubMed: 19917928]
8. Gubanova E, Brown B, Ivanov SV, Helleday T, Mills GB, Yarbrough WG, et al. Downregulation of SMG-1 in HPV-positive head and neck squamous cell carcinoma due to promoter hypermethylation correlates with improved survival. Clin Cancer Res. 2012; 18:1257–67. [PubMed: 22247495]
9. DeWeese TL, Walsh JC, Dillehay LE, Kessis TD, Hedrick L, Cho KR, et al. Human papillomavirus E6 and E7 oncoproteins alter cell cycle progression but not radiosensitivity of carcinoma cells treated with low-dose-rate radiation. Int J Radiat Oncol Biol Phys. 1997; 37:145–54. [PubMed: 9054890]
10. Nichols AC, Yoo J, Palma DA, Fung K, Franklin JH, Koropatnick J, et al. Frequent mutations in TP53 and CDKN2A found by next-generation sequencing of head and neck cancer cell lines. Arch Otolaryngol Head Neck Surg. 2012; 138:732–9. [PubMed: 22911296]
11. Stransky N, Egloff AM, Tward AD, Kostic AD, Cibulskis K, Sivachenko A, et al. The mutational landscape of head and neck squamous cell carcinoma. Science. 2011; 333:1157–60. [PubMed: 21798893]
12. Agrawal N, Frederick MJ, Pickering CR, Bettegowda C, Chang K, Li RJ, et al. Exome sequencing of head and neck squamous cell carcinoma reveals inactivating mutations in NOTCH1. Science. 2011; 333:1154–7. [PubMed: 21798897]
13. Wise-Draper TM, Wells SI. Papillomavirus E6 and E7 proteins and their cellular targets. Front Biosci. 2008; 13:1003–17. [PubMed: 17981607]
14. Shin MK, Pitot HC, Lambert PF. Pocket proteins suppress head and neck cancer. Cancer Res. 2012; 72:1280–9. [PubMed: 22237625]
15. Jabbar S, Strati K, Shin MK, Pitot HC, Lambert PF. Human papillomavirus type 16 E6 and E7 oncoproteins act synergistically to cause head and neck cancer in mice. Virology. 2010; 407:60–7. [PubMed: 20797753]
16. Strati K, Lambert PF. Role of Rb-dependent and Rb-independent functions of papillomavirus E7 oncogene in head and neck cancer. Cancer Res. 2007; 67:11585–93. [PubMed: 18089787]
17. Pfister DG, Ang KK, Brizel DM, Burtness BA, Cmelak AJ, Colevas AD, et al. National Comprehensive Cancer Network Clinical Practice Guidelines in Oncology. Head and neck cancers. J Natl Compr Canc Netw. 2011; 9:596–650. [PubMed: 21636536]
18. James MA, Lee JH, Klingelhutz AJ. HPV16-E6 associated hTERT promoter acetylation is E6AP dependent, increased in later passage cells and enhanced by loss of p300. Int J Cancer. 2006; 119:1878–85. [PubMed: 16708385]
19. Kimple R, Vaseva A, Cox A, Baerman K, Calvo B, Tepper J, et al. Radiosensitization of pancreatic cancer cells via Akt inhibition. Clinical Cancer Research. 2010; 16:912–23. [PubMed: 20103665]
20. Steenbergen RD, Hermsen MA, Walboomers JM, Joenje H, Arwert F, Meijer CJ, et al. Integrated human papillomavirus type 16 and loss of heterozygosity at 11q22 and 18q21 in an oral carcinoma and its derivative cell line. Cancer Res. 1995; 55:5465–71. [PubMed: 7585617]
21. Ferris RL, Martinez I, Sirianni N, Wang J, Lopez-Albaitero A, Gollin SM, et al. Human papillomavirus-16 associated squamous cell carcinoma of the head and neck (SCCHN): a natural disease model provides insights into viral carcinogenesis. Eur J Cancer. 2005; 41:807–15. [PubMed: 15763658]
22. Bradford CR, Zacks SE, Androphy EJ, Gregoire L, Lancaster WD, Carey TE. Human papillomavirus DNA sequences in cell lines derived from head and neck squamous cell carcinomas. Otolaryngol Head Neck Surg. 1991; 104:303–10. [PubMed: 1851275]
23. Ballo H, Koldovsky P, Hoffmann T, Balz V, Hildebrandt B, Gerharz CD, et al. Establishment and characterization of four cell lines derived from human head and neck squamous cell carcinomas for an autologous tumor-fibroblast in vitro model. Anticancer Res. 1999; 19:3827–36. [PubMed: 10628319]
24. Pyeon D, Newton MA, Lambert PF, den Boon JA, Sengupta S, Marsit CJ, et al. Fundamental differences in cell cycle deregulation in human papillomavirus-positive and human

papillomavirus-negative head/neck and cervical cancers. Cancer Res. 2007; 67:4605–19. [PubMed: 17510386]

25. Chen AM, Li J, Beckett LA, Zhara T, Farwell G, Lau DH, et al. Differential response rates to irradiation among patients with human papillomavirus positive and negative oropharyngeal cancer. Laryngoscope. 2012
26. Amundson SA, Do KT, Vinikoor LC, Lee RA, Koch-Paiz CA, Ahn J, et al. Integrating global gene expression and radiation survival parameters across the 60 cell lines of the National Cancer Institute Anticancer Drug Screen. Cancer Res. 2008; 68:415–24. [PubMed: 18199535]
27. Wald AI, Hoskins EE, Wells SI, Ferris RL, Khan SA. Alteration of microRNA profiles in squamous cell carcinoma of the head and neck cell lines by human papillomavirus. Head Neck. 2011; 33:504–12. [PubMed: 20652977]
28. Lin CJ, Grandis JR, Carey TE, Gollin SM, Whiteside TL, Koch WM, et al. Head and neck squamous cell carcinoma cell lines: established models and rationale for selection. Head Neck. 2007; 29:163–88. [PubMed: 17312569]
29. Moody CA, Laimins LA. Human papillomavirus oncoproteins: pathways to transformation. Nat Rev Cancer. 2010; 10:550–60. [PubMed: 20592731]
30. Hampson L, El Hady ES, Moore JV, Kitchener H, Hampson IN. The HPV16 E6 and E7 proteins and the radiation resistance of cervical carcinoma. FASEB journal: official publication of the Federation of American Societies for Experimental Biology. 2001; 15:1445–7. [PubMed: 11387252]
31. Nigro ND, Seydel HG, Considine B, Vaitkevicius VK, Leichman L, Kinzie JJ. Combined preoperative radiation and chemotherapy for squamous cell carcinoma of the anal canal. Cancer. 1983; 51:1826–9. [PubMed: 6831348]
32. Green JA, Kirwan JM, Tierney JF, Symonds P, Fresco L, Collingwood M, et al. Survival and recurrence after concomitant chemotherapy and radiotherapy for cancer of the uterine cervix: a systematic review and meta-analysis. Lancet. 2001; 358:781–6. [PubMed: 11564482]
33. Kimple RJ, Harari P, Torres AD, Yang RZ, Soriano BJ, Yu M, et al. Development and characterization of HPV-positive and HPV-negative head and neck squamous cell carcinoma tumorgrafts. Clinical Cancer Research. 2013; 19:855–64. [PubMed: 23251001]
34. Bykov VJ, Issaeva N, Shilov A, Hultcrantz M, Pugacheva E, Chumakov P, et al. Restoration of the tumor suppressor function to mutant p53 by a low-molecular-weight compound. Nat Med. 2002; 8:282–8. [PubMed: 11875500]

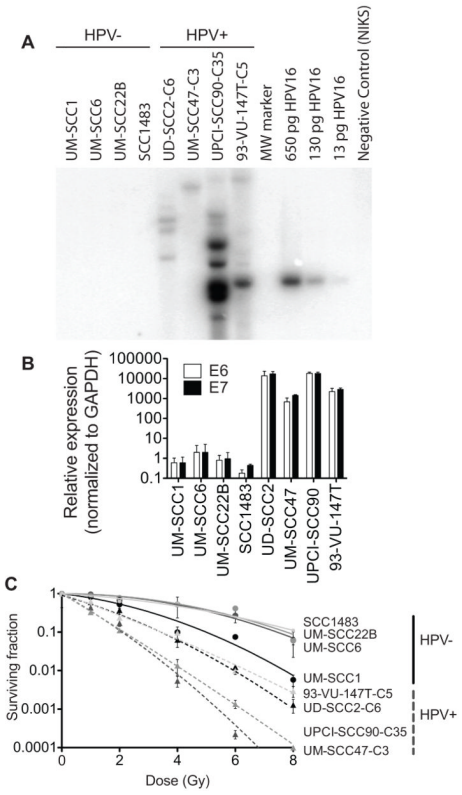

Figure 1.

A) HPV-16 specific Southern blot of cell lines used confirmed the presence of HPV-16 DNA in UD-SCC2, UM-SCC47, UPCI-SCC90, and 93-VU-147T, but not UM-SCC1, UM-SCC6, UM-SCC22B, or SCC1483. C# refers to the clone number of each individual clonal population utilized. B) Quantitative RT-PCR of total cellular RNA for *HPV-16 E6* and *E7* confirmed the presence of RNA encoding *HPV-16 E6* and *HPV-16 E7* in HPV+, but not HPV− cells. Data shown are mean expression +/− SEM (each sample normalized to *GAPDH*) from three biologic replicates each run as three technical replicates. C. Increased radiation sensitivity in HPV-positive head and neck cancer cells. Clonogenic survival over a range of radiation doses for HPV+ cells (dashed lines, triangles) and HPV− (solid lines, circles) demonstrate significantly increased radiation sensitivity in HPV+ cells (n=6 per condition). Mean surviving fraction after 2 Gy is 22% for HPV+ vs. 59% for HPV− cells ($p<0.0001$).

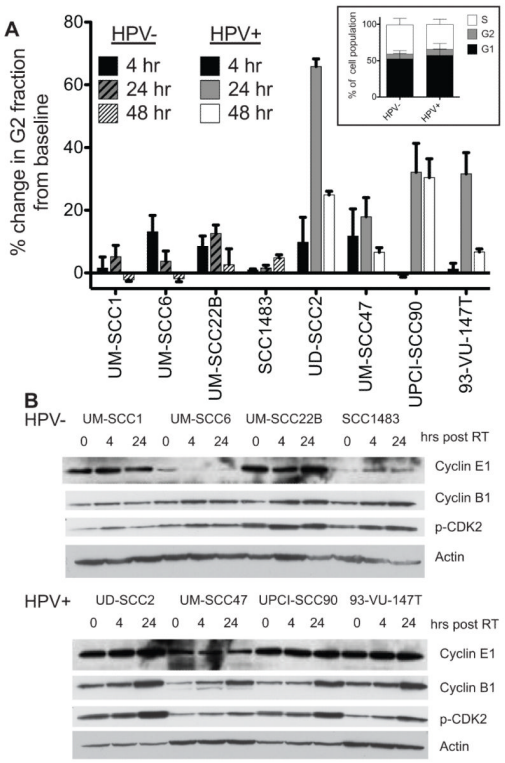

Figure 2.

Radiation induced G2/M cell cycle arrest in HPV+ HNC. A) Absolute change in percentage of cells in G2/M at indicated time points after radiation (4 Gy) as assessed by propidium iodide staining and flow cytometry assessment. The baseline fraction of cells in G2/M is subtracted from indicated mean (n=3) population distribution. Inset: No difference in baseline cell cycle distribution between HPV+ and HPV− cells is observed. B) Immunoblot analysis showing activation of Cyclin B1 and phospho-CDK2, but not Cyclin E1 in HPV+ HNC cells following radiation (4 Gy).

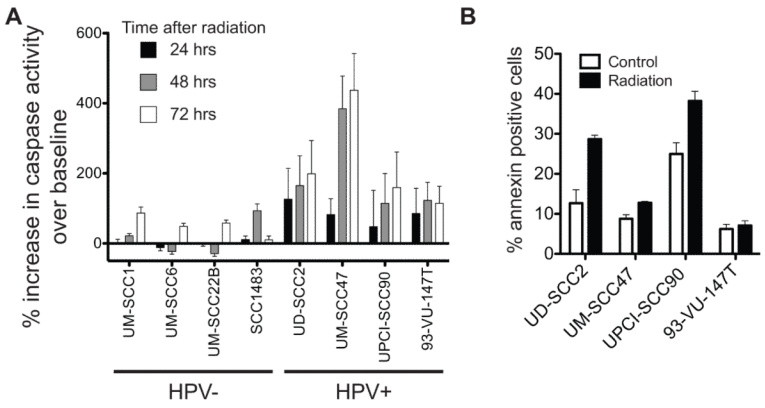

Figure 3.

Apoptosis in HPV+ HNC after radiation. A) Significantly increased caspase activity compared to baseline, unirradiated cells, was seen in HPV+, but not HPV− HNC. Shown is the mean percentage increase in caspase activity over baseline as measured by luminescent caspase activation assay at indicated times following a single 4 Gy dose of radiation (n=4-6 per condition). B) Annexin V and propidium iodide staining to identify an apoptotic population of cells demonstrated a significant increase in the proportion of cells in apoptosis (early + late) following a single 4 Gy dose of radiation in HPV+ HNC cells (n=3, 2-way ANOVA, $p<0.0001$).

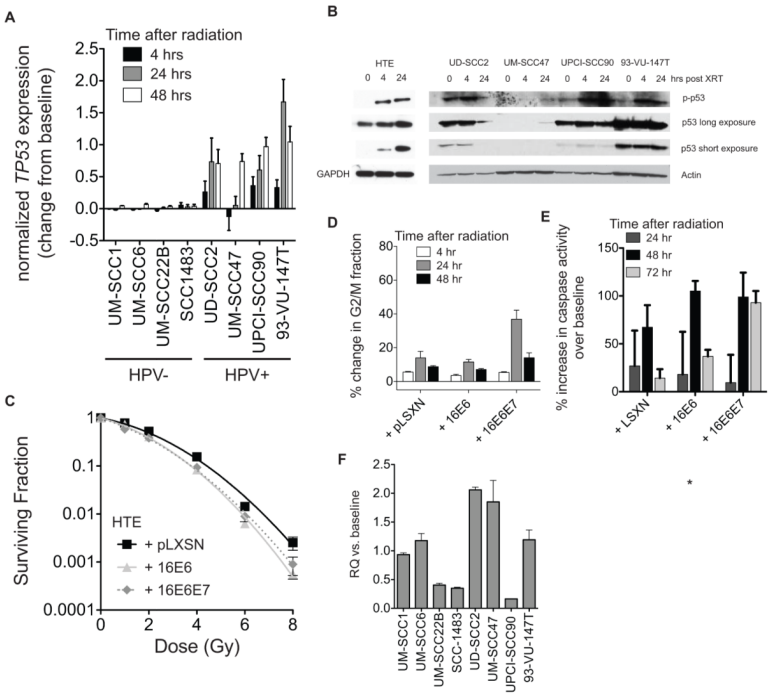

Figure 4.

HPV16 E6 modulation of radiation response. A) Increased *TP53* RNA following radiation in HPV+ HNC cells. Data presents *TP53* expression at indicated time points, normalized to unirradiated control cells for each individual cell line. B) Increased phospho- and total-p53 protein is seen in HPV+ HNC following radiation. Low levels of p53 in several cell lines necessitated prolonged exposures to identify protein bands. 25 μg of total protein was loaded into each well. C) The clonogenic capacity of human tonsillar epithelial (HTE) cells stably expressing vector alone (black squares, HPV-16 E6 (grey triangles) or HPV-16 E6/E7 (grey diamonds) was assessed by colony formation assay over a range of radiation doses showing that expression of HPV-16 E6 resulted in increased sensitivity to radiation. D) Increase in G2/M fraction in HPV16 E6 and E6/E7 expressing cells relative to baseline, unirradiated cells. Absolute change in percentage of cells in G2/M at indicated time points after radiation (4 Gy) as assessed by propidium iodide staining and flow cytometry assessment. The baseline fraction of cells in G2/M is subtracted from indicated mean (n=3) population distribution. E) Significantly increased caspase activity as measured by substrate cleavage compared to baseline, unirradiated cells, was seen in HPV16 E6 and E6/E7 expressing cells. F) 24 h after radiation, increased p21 RNA was detected by qRT-PCR in HPV+, but not HPV−, cells.

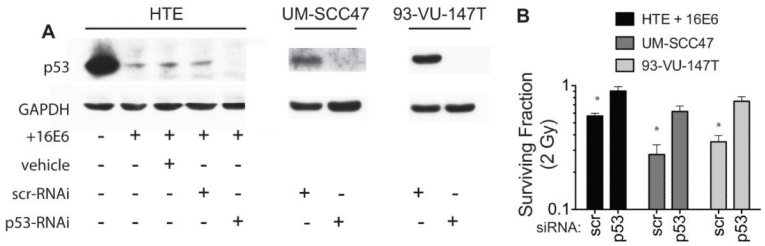

Figure 5.

Critical role for p53 in radiation response of HPV+ HNC. A) Expression of HPV16 E6 results in decreased detectable p53 protein while use of p53 specific siRNA, but not scrambled or vehicle control, results in further loss of p53 expression in HTE HPV16 E6 expressing cells (left, 25 μg of total protein), UM-SCC47 cells (center, 75 μg of total protein) and 93-VU-147T cells (right, 25 μg of total protein). E) Knockdown of *TP53* causes greater colony formation HTE +16E6, UM-SCC47, and 93-VU-147T cells (n=6 per condition). Compared to unirradiated cells the surviving fraction of scrambled siRNA pretreated cells was significantly lower than that of TP53 specific siRNA treated cells (*$p<0.0001$).

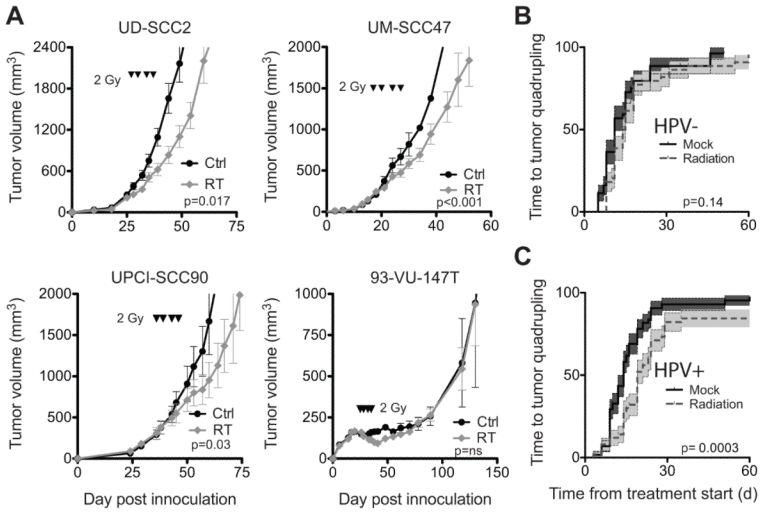

Figure 6.

Increased radiation sensitivity observed in vivo using xenograft model system. Mice (n=10/condition) implanted with indicated cell lines (1×10^6/site) in bilateral flanks were treated with four fractions of radiation (2 Gy) delivered over 2 weeks. Tumor volumes were measured, mean tumor volume +/− SEM is shown and curves were fit to an exponential growth equation and compared by the extra sum-of-squares f-test. Time to tumor quadrupling was calculated from the first day of treatment and graphed according to the Kaplan-Meier method. Curve comparisons for control vs. radiation treated mice were performed with the log-rank (Mantel Cox) test. A) HPV+ cell lines showed growth delay following radiation in 3 of 4 cell lines. B) No significant difference in time to tumor quadrupling was seen between control and radiation treated HPV− xenografts using the indicated treatment schedule (p=0.14). C) Radiation resulted in a significant delay in tumor quadrupling for HPV+ cells (p=0.0003).

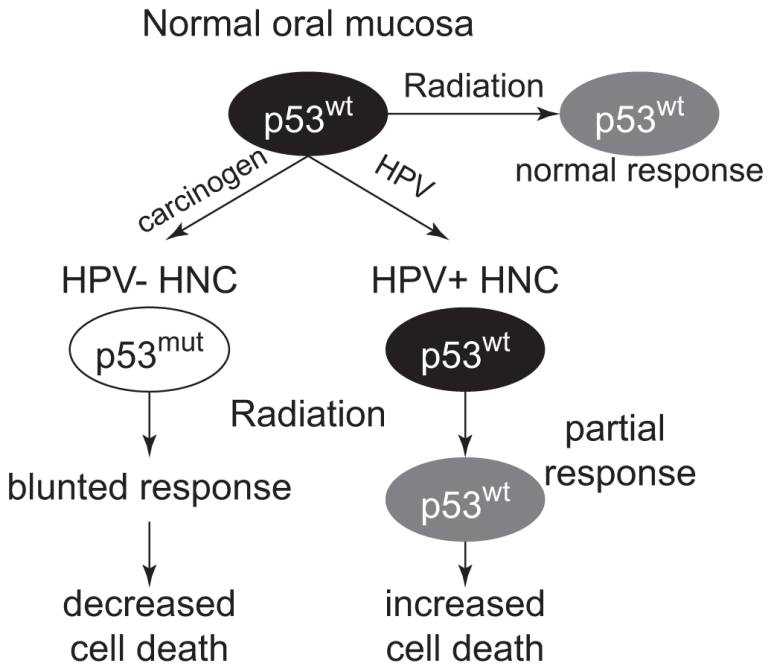

Figure 7.
Proposed model underlying increased sensitivity to radiation in HPV+ HNC. In HPV− HNC, mutations in either TP53, or alteration in p53 signaling bypass the cell cycle arrest typically induced following radiation. While HPV E6 in HPV+ HNC degrades p53, low levels of wild-type p53 remain and can be activated by radiation-induced DNA damage resulting in partial arrest and increased cell death.